

Amplitudes for One-way Extrapolators

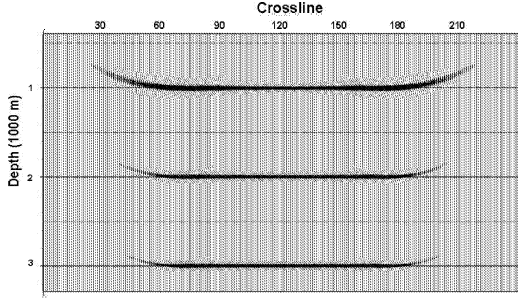


Fig. 3: Flat reflectors along the center inlines after 3-D common shot migration.

we see that the modified initial condition for U gives an additional phase shift $i\omega$. We also need to modify the imaging condition to be

$$R(x, y, z) = \int \frac{\hat{p}_U(x, y, z; \omega)}{\hat{p}_D(x, y, z; \omega)} d\omega. \quad (12)$$

Here p_D and p_U are defined as

$$p_D = \Lambda^{-1}D, \quad p_U = \Lambda^{-1}U,$$

which satisfy $p_D + p_U = p$. It is easy to see p_U and p_D are downgoing and upgoing waves (p^+ and p^-) introduced in Wapenaar (1998). Noticing $\lambda = i\frac{\omega}{v} \cos \alpha$ and applying stationary phase to (11) and (12), we obtain

$$R(x, y, z) \sim \iiint \frac{\cos \alpha_{r0}}{v_0} \sqrt{\frac{\cos \alpha_s \psi_s \sigma_s}{\cos \alpha_r \psi_r \sigma_r}} e^{i\omega(\tau_r + \tau_s)} \hat{Q} dx_r dy_r d\omega. \quad (13)$$

For constant velocity, the splitting (10) is exact. Therefore (11) and imaging condition (12) give the true-amplitude result. This can be directly seen by comparing (13) with (3) and setting $\alpha_{s0} = \alpha_s$, $\alpha_{r0} = \alpha_r$. For the $v(z)$ case, we need to apply another correction term

$$\sqrt{\frac{\cos \alpha_{s0} \cos \alpha_r}{\cos \alpha_s \cos \alpha_{r0}}},$$

or

$$\sqrt{\frac{\lambda_{s0} \lambda_r}{\lambda_s \lambda_{r0}}}.$$

Research is currently in progress on modifying the differential operators in (10) to include this factor in the resulting D and U .

Numerical results

Figure 2 (left) shows the 3-D migrated impulse responses along the center inline from a trace with three 7.5 Hz

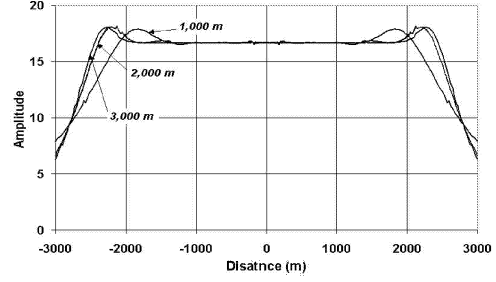


Fig. 4: Peak migrated amplitudes of the three reflectors in Figure 3.

Ricker wavelets at depth 1000m, 2000m and 3000m, respectively. The source is at crossline 121 and receiver at crossline 141 and trace spacing is 50m in both inline and crossline directions. The medium velocity is 2000m/s. Unlike the kinematic behavior, the amplitudes of the impulse responses are asymmetric, with a bias on the receiver side. The peak amplitudes along the impulse responses are in good agreement with the theoretical prediction shown in Figure 2 (right).

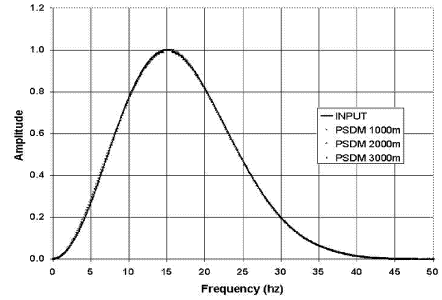


Fig. 5: Frequency spectrum of the migrated wavelets at inline 121 and crossline 121. The solid line is the spectrum of the input 15 Hz Ricker wavelet. The overlay is nearly perfect.

Figure 3 is the center inline of the 3-D migrated result from a single shot over three flat reflectors. The peak amplitudes along the three migrated reflectors are shown in Figure 4. Aside from the edge effects and small jitters caused by interference with wraparound artifacts, the 3-D common shot migration recovers the reflectivity accurately. Figure 5 shows that the frequency content is preserved by the migration at the center trace location. However, the wavelet becomes progressively lower frequency away from the center trace due to the effects of stretching and anti-aliasing.

The next example is from the 3-D SEG-EAGE salt model. The “area shot” dataset was selected over the marine streamer C3-NA dataset because of size considerations. However, this “area shot” dataset is known to produce